Classification of electrically-evoked compound action potentials in the parkinsonian subthalamic nucleus of non-human primates

Joshua Rosing[a], Alex Doyle[b], AnneMarie Brinda[a], Madeline Blumenfeld[a], Emily Lecy[b], Chelsea Spencer[a], Joan Dao[a], Jordan Krieg[a], Kelton Wilmerding[a], Disa Sullivan[a], Sendréa Best[a], Biswaranjan Mohanty[c], Jing Wang[c], Luke A. Johnson[c], Jerrold L. Vitek[c], and Matthew D. Johnson[a]

[a]Department of Biomedical Engineering, University of Minnesota, Minneapolis, MN, USA
[b]Department of Neuroscience, University of Minnesota, Minneapolis, MN, USA
[c]Department of Neurology, University of Minnesota, Minneapolis, MN, USA

Short Title: Mapping ECAPs in the STN

Corresponding author:

Matthew D. Johnson
Department of Biomedical Engineering
University of Minnesota
6-134 Nils Hasselmo Hall
312 Church Street SE
Minneapolis, MN 55455

Email: john5101@umn.edu
Phone: 612-626-6492

Abstract

Background. Electrically evoked compound action potentials (ECAPs) generated in the subthalamic nucleus (STN) contain features that may be useful for titrating deep brain stimulation (DBS) therapy for Parkinson's disease. While previous studies have leveraged macroscale DBS electrodes, directional DBS leads with split-band contacts are thought to enable sampling ECAPs at a higher spatial resolution both within and adjacent to the STN.

Objective. In this study, we investigated the spatiotemporal features of ECAPs in and around the STN across parameter sweeps of stimulation current amplitude, pulse width, and electrode configuration.

Methods. Four non-human primates were implanted unilaterally with either a directional (n=3) or non-directional (n=1) DBS lead targeting the sensorimotor STN. Resting-state ECAPs were recorded before and after rendering the subjects parkinsonian with MPTP treatments.

Results. ECAP responses were characterized by primary features (within 1.6ms after a stimulus pulse) and secondary features (between 1.6-7.4ms after a stimulus pulse). Using these ECAP features, a linear classifier was able to differentiate electrodes within and dorsal to the STN in all four subjects.

Conclusion. ECAP responses varied systematically with recording and stimulating electrode location, which may provide utility in efficiently defining DBS electrode configurations to target pathways in and around the STN for treating symptoms of Parkinson's disease.

1. Introduction

Electrical stimulation within the nervous system is well known to generate ECAPs whose features occur within milliseconds of stimulus onset and attenuate in amplitude over time [1,2]. This physiological activity, which is often detected from one or more recording electrodes positioned near the stimulating electrode, reflects the spatial summation of induced membrane polarization adjacent to the recording electrode(s) [3–6]. ECAP features are thought to be indicative of both direct activation of axons (immediate primary features) as well as synaptic and network-level modulation patterns (delayed secondary features) [1,2].

Such ECAP features have shown utility for assessing the degree of membrane polarization and thus target engagement with peripheral nerve [7], spinal cord [8–10], cochlear [11–14], retinal [15,16], and deep brain [2,17] stimulation. ECAP features have also been integrated as feedback signals to adjust therapies dynamically, including cochlear implants to streamline behavioral fitting procedures [18] and spinal cord stimulation to account for changes in the distance between the stimulating electrode(s) and the spinal cord during activities of daily living [9].

Similarly, for DBS applications, knowing the spatial position and orientation of each electrode in the context of the targeted nucleus or fiber pathways can be helpful for fine-tuning stimulation settings [19]. Previous studies have shown that ECAP feature presence and prominence in the STN is associated with therapeutic effectiveness in Parkinson's disease [17,20]. However, the degree of spatial heterogeneity of ECAPs within and adjacent to the STN remains unclear. In this study, we investigated the spatiotemporal features of ECAPs in and around the STN in four non-human primates rendered parkinsonian with MPTP treatments.

2. Methods

2.1. Animals

This study investigated ECAPs from STN-DBS leads in four aged female rhesus macaque monkeys (*macaca mulatta*; Subjects Ne, Az, So, and Bl; 14.75, 18.5, 19.5, and 26 years old, respectively, at the time of the recordings). Procedures used in the study were approved by the University of Minnesota's Institutional Animal Care and Use Committee and were performed following the United States Public Health Service policy for humane care and use of laboratory animals. All animals received environmental enrichment, free access to water, and a wide variety of foods, including fresh fruits and vegetables. All effort was made to provide animals with adequate care and prevent discomfort during the study.

2.2. Surgical Procedures

Animals were imaged pre-operatively using a 7T or 10.5T human bore magnet with custom-designed head coils for non-human primates at the Center for Magnetic Resonance Research at the University of Minnesota. Similar to previous studies [21,22], DBS leads were implanted along an oblique mapping track that had the largest span of sensorimotor-responsive STN cell activity. The depth of the implant was designed to have electrodes within the sensorimotor STN and the region dorsal to the STN, containing the lenticular fasciculus [23] (**Fig. 1**).

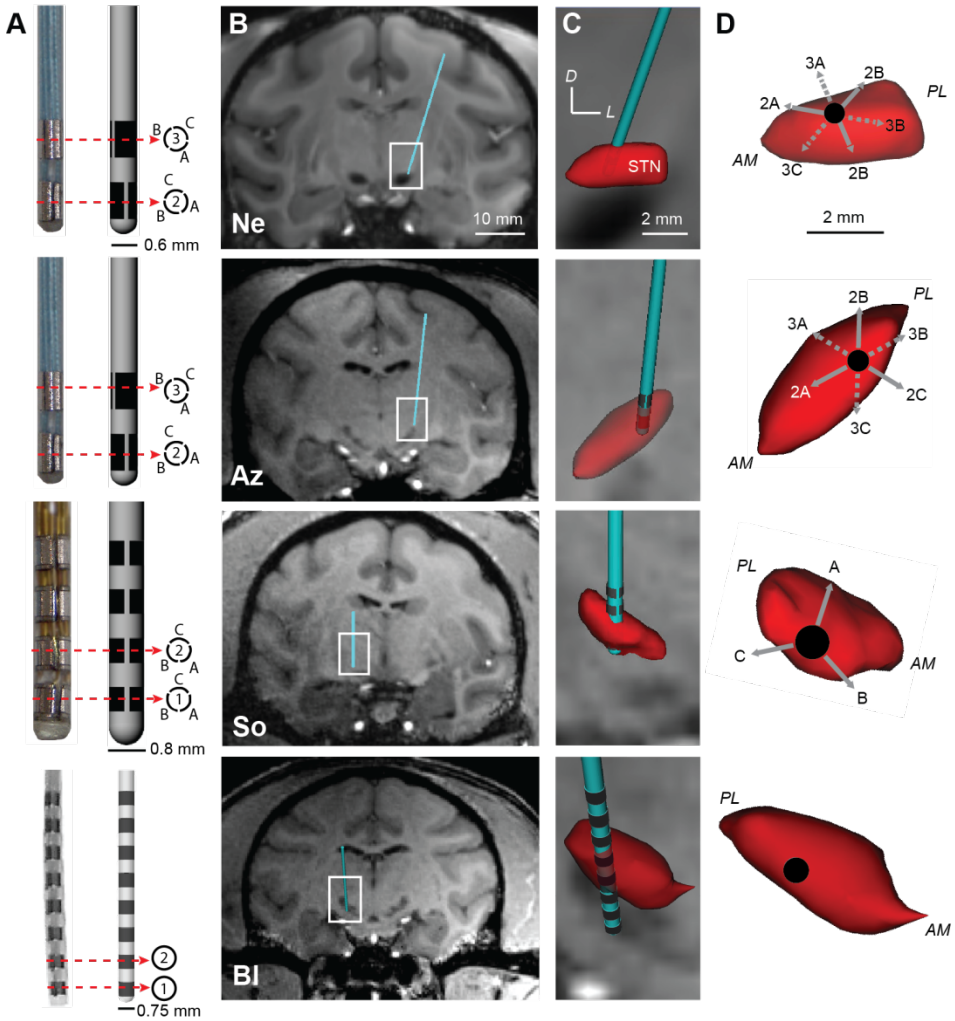

Figure 1. DBS lead localization within the STN. (A) Directional and non-directional DBS leads used in this study. (B, C) High-field 7T MRI and CT co-registration were used to identify the position of each lead within the subthalamic nucleus with confirmation from post-mortem block-face histology. (D) Oblique perspective of the DBS lead implant showing the position of each lead within the STN and the orientation of the segmented row electrodes, if present. Spatial positions are shown with antero-medial (AM) and postero-lateral (PL) indicators.

2.3. DBS Implant Procedures

Subjects Ne and Az were implanted with a 6-channel directional DBS lead (Abbott Neuromodulation, 0.6mm diameter), consisting of 2 rows and 3 columns of electrodes (0.75mm height, 0.5mm spacing between rows) with the top row clocked 60 degrees from the bottom row. Subject So was implanted with a 12-channel directional DBS lead (Heraeus Medical Components, 0.8mm diameter), consisting of 4 rows and 3 columns of electrodes (0.5mm height, 0.5mm spacing) with no rotational offset. Subject Bl was implanted with a non-directional DBS lead (NuMed, 0.625mm diameter) with 8 electrodes (one band electrode per row, 0.5mm height, and 0.5mm spacing). DBS lead wires were routed to another chamber to interface with an external neurostimulator (IZ2MH) and recording (PZ5) system (Tucker-Davis Technologies). A CT scan

was taken post-implant and co-registered to the pre-operative MRI to estimate placement of the DBS lead implant with respect to the STN (**Fig. 1**), and this was confirmed with post-mortem block-face histological imaging. Split-band electrode orientation for Subjects Ne, Az, and So was determined using a post-mortem bubble test whereby the explanted lead, still integrated with the chamber and cap, was submerged in 0.9% saline and stimulated through with 1-5mA DC current over 1-5sec to generate an electrolysis reaction and small bubble at the stimulated electrode. This was used to verify electrode connector maps, check for electrical shorts, and identify each electrode's orientation relative to the brain.

2.4. ECAP Stimulation Protocol

Monopolar stimulus pulse trains (125Hz) were delivered through a single electrode contact using biphasic pulse waveforms that alternated between cathodic and anodic for first phase polarities. The first phase had a duration of 100µs, and the second active recharge phase had a duration of 1ms with a stimulus amplitude at 10% of the first phase's amplitude. Using these waveforms and pulse trains, the overall stimulus amplitude was increased until sustained side effects were observed on the contralateral side (e.g., muscle contractions, dyskinesias, etc.). Subsequent stimulation trials were then capped at 25µA below the side effect threshold as determined for each electrode on the DBS lead, except in one case (Subject So) where ECAPs were recorded transiently at higher amplitude settings during dyskinesias. During all stimulation trials, wide-band, monopolar ECAP recordings were collected from the other electrodes at a sampling rate of 48.8kHz and in reference to cranial bone screws distributed over the parietal lobe.

2.4.1. Current Sweep Experiments

To confirm the existence of ECAPs as neural responses as opposed to electrical artifacts, the current amplitude of the stimulus pulse train was varied randomly between 0µA and 25µA below the side effect threshold for each electrode. Current sweep data collection trials consisted of 5 seconds of stimulation followed by 5 seconds of no stimulation at each amplitude, with repeated measures of 5 trials per electrode. To compare results amongst subjects (Ne and Bl), all current sweep data were collected in a parkinsonian condition.

2.4.2. Strength-Duration Sweep Experiments

To further confirm that the signals were of neural origin, strength-duration relationships were assessed through ECAP recordings by systematically varying the current amplitude and pulse width of the first phase of the charge-balanced, biphasic waveform. The protocol consisted of stimulating at (1) seven current amplitudes (12.5%, 25%, 37.5%, 50%, 62.5%, 75% and 87.5% of side-effect threshold) in the parkinsonian condition, and (2) five pulse widths per stimulus amplitude ranging from 40 to 160µs for the first phase. Each trial consisted of 30sec of stimulation followed by 30sec without stimulation for each parameter combination. The presentation order of the parameters was randomized but kept consistent across electrodes and subjects (Az and So).

2.5. MPTP Treatment and Evaluation

Each primate was given a series of systemic injections of the neurotoxin MPTP (1-methyl-4-phenyl-1,2,3,6-tetrahydropyridine). Following MPTP treatment, the parkinsonian motor sign severity was rated for each subject using a modified version of the Unified Parkinson's Disease Rating Scale (mUPDRS), which consisted of 14 motor scores, quantified from 0 (no effect) to 3 (severe) [24]. The total motor score for each subject was used to determine the overall severity of

parkinsonian motor signs, and these scores were measured at least five times. Averaged scores were 18.25/42 for Subject Ne (moderate), 8.47/42 for Subject Az (mild), 0/42 for Subject So (asymptomatic), and 10.4/27 for Subject Bl (moderate).

2.6. ECAP Processing

Data collected during current sweep and strength-duration sweep experiments were processed to remove the stimulation artifacts and residual noise (**Fig. 2**). First, baseline subtraction was applied to each interstimulus ECAP segment (8ms long) by subtracting the amplitude of the first data point (0.4ms before the stimulus pulse) from all subsequent data points in the ECAP segment. Next, segments were sorted based on cathodic-anodic or anodic-cathodic stimulus waveforms to ensure that the sample sizes for both stimulus waveforms were identical. For the current sweep experiments, all 5sec of ECAP recordings were averaged together, and for the strength-duration sweep experiments, only the last 20sec of the 30sec long ECAP recordings were averaged together. Averaging significantly reduced the electrical artifact as shown in **Fig. 2**. The resulting data were then smoothed (4-sample moving average over the first 1.17ms and 16 sample moving average over the remaining portion of the segment). This two-part filtering approach avoided over-smoothing the primary features while still removing high frequency noise from the secondary features of the ECAP.

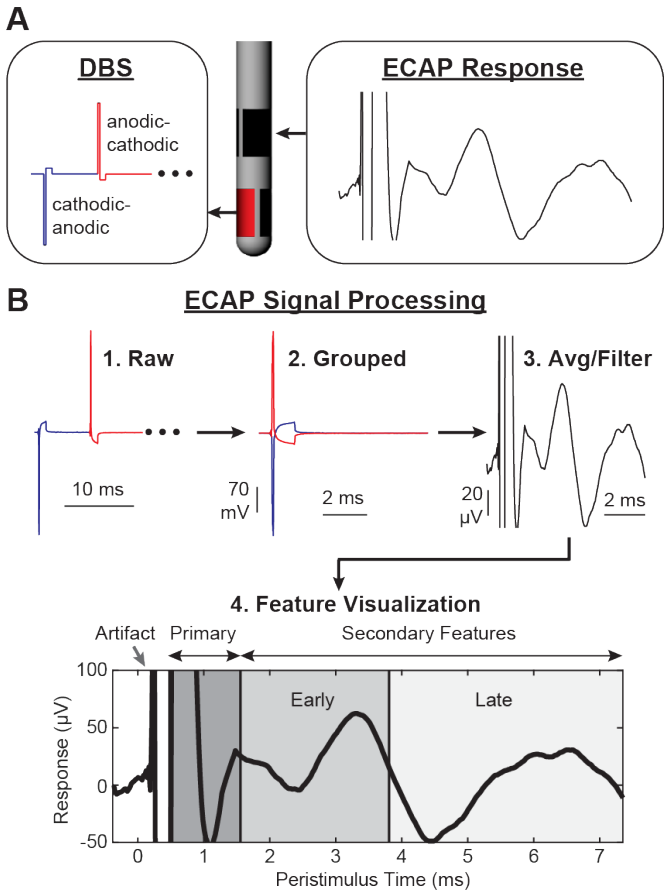

Figure 2. Signal processing of ECAPs within and adjacent to the STN. (A) An alternating sequence of cathodic-leading and anodic-leading waveforms was applied through one electrode while ECAP recordings were collected through all adjacent electrodes. (B) Raw ECAP data were

grouped, averaged, filtered, and separated into primary, early secondary, and late secondary features.

Some ECAP recordings, most notably in Subjects Az and So, contained a 0.8-1.0kHz noise source that was consistent in amplitude over the entire peri-stimulus time window. The peri-stimulus data (from 1.25-7.4ms) was passed through an IIR filter with 0.99 steepness, with the delayed filter onset designed to avoid generating artifacts in the primary features. The processed data before and after 1.25ms were then stitched together with a weighted averaging of 9 samples about the stitch to avoid discontinuities in the data (sample 1 was 90% unfiltered sample value plus 10% filtered sample value, and sample 9 was 10% unfiltered sample value plus 90% filtered sample value).

Data with this 0.8-1.0 kHz noise source were marked for filtering objectively as follows. The maximum spectral power in two bands (<500Hz and 700-1500Hz) in each recording were calculated and used to define to conditions: (A) the maximum spectral power of the unfiltered <500Hz band was sufficiently greater (determined by a manually set threshold for each subject) than the maximum spectral power for the unfiltered 700-1500Hz band, and (B) the maximum spectral power of the unfiltered <500Hz band was less than the maximum spectral power of the filtered <500Hz band. If condition A was false, or if both conditions were true, the recording was marked for filtering.

2.7. Data Analysis and Classification

ECAP feature windows were determined based on time segments containing similar ECAP responses within and across subjects. Primary features were the first positive and negative peaks to occur, typically within 0.6-1.6 ms of stimulus pulse onset. Secondary features were divided into early (1.6-3.8 ms) and late (3.8-7.4 ms) windows after a stimulus pulse. The separation between early and late windows was based on the transition between stimulus evoked neuronal spike inhibition and a return to a baseline spiking probability with peri-stimulus firing rates of STN neurons during STN-DBS (see [25]). For each ECAP window, the root mean square (RMS) of the data was calculated and then used as feature amplitudes for graphical comparisons, and as features in a linear discriminant analysis classifier. The rationale for feature windows as opposed to defining specific peaks and troughs was based on observations that ECAP features differed in manifestation and in their exact timing across recording configurations for each subject.

2.7.1. Classifier Accuracy

A linear classifier (MATLAB 'classify') was used to predict stimulation and recording electrode site locations for two possible groups – STN/STN and ThF/ThF (thalamic fasciculus) – in all subjects. The classifier used all data points from those two groups as samples and training in a leave-one-out approach. Accuracy was calculated from the classification error, was averaged across trials, and compared against chance (50%) to determine effectiveness of the classifier. Additionally, the classifier was used to test each subject against three training subjects. In this case, the classifier was trained using all data from the three training subjects and tested using all data from the fourth subject.

2.7.2. Peak and Trough Amplitudes and Timings

To more precisely depict the changes of ECAP feature responses to increases in stimulation amplitude, MATLAB's findpeaks() function was used to capture peak and trough amplitudes and

time locations. The trough amplitude was subtracted from the peak amplitude to find a peak-trough amplitude. The timings of each peak and trough pair were averaged to find each peak-trough timing.

3. Results

3.1. Distributions and Variability of ECAP Features

Within-subject comparison of ECAPs across all stimulation parameters showed high variability of responses (**Fig. 3**). Variance was highest during the period of known artifact, and second highest during the earlier portion of the primary feature window. The primary feature window's variance formed a second peak, suggesting a different source than that of the artifact's variance. Variance declined rapidly during the primary feature window for most subjects, then steadily declined over the early and late secondary feature windows. Most subjects showed much lower variance during the secondary feature windows than during the primary feature window.

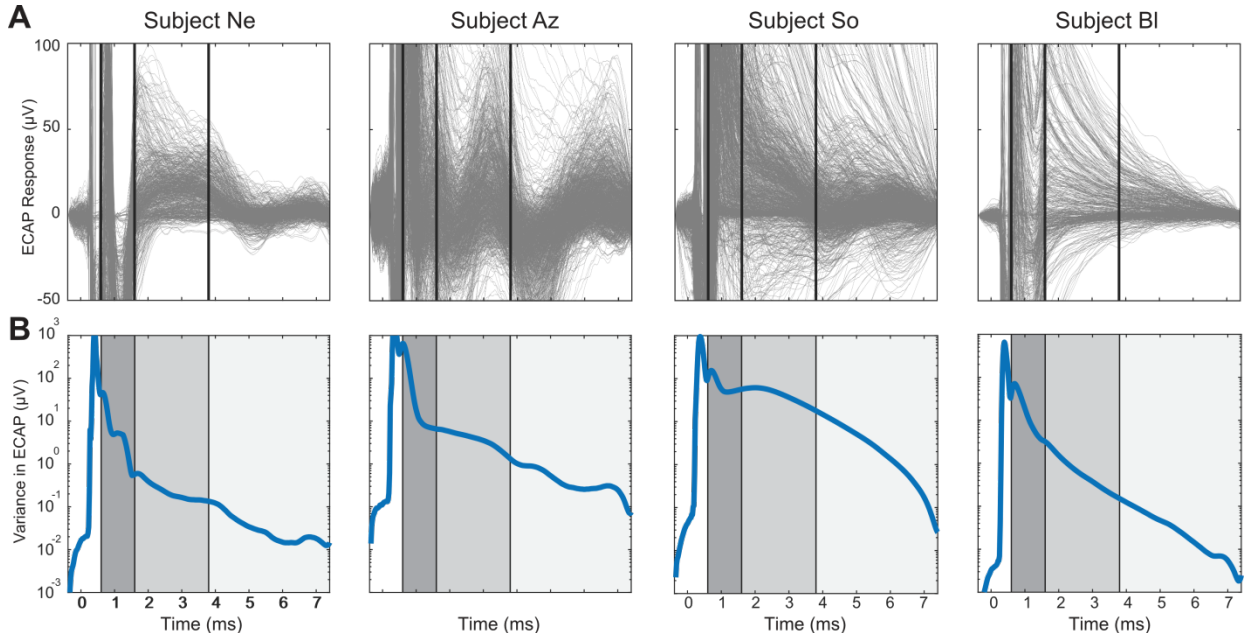

Figure 3. Distributions of all ECAP recordings across subjects. (A) Pooled recordings across tested stimulation pulse widths (subjects Az and So only), amplitudes (all subjects), and electrode configurations (all subjects) for a single recording day. (B) Variance across pooled recordings across the ECAP window. Black lines indicate edges of selected feature windows (primary: 0.6-1.6ms, early secondary 1.6-3.8ms, late secondary 3.8-7.4ms).

3.2. ECAP Responses to Varying Stimulation Amplitudes and Pulse Widths

Current sweep and pulse width sweep experiments in each of four subjects showed that features of the ECAP response changed non-linearly to adjustments in stimulation parameters while the unfiltered stimulation artifact increased linearly with stimulation amplitude and pulse width (**Fig. 4 and 5**), negating the possibility that they are artificial. Features emerged gradually as stimulation amplitude was increased, with secondary features appearing only at stimulation amplitudes that were higher than those sufficient to evoke primary features (**Fig. 4**). Primary and secondary

features also generally increased in amplitude with increasing stimulation amplitude (**Fig. 4**).

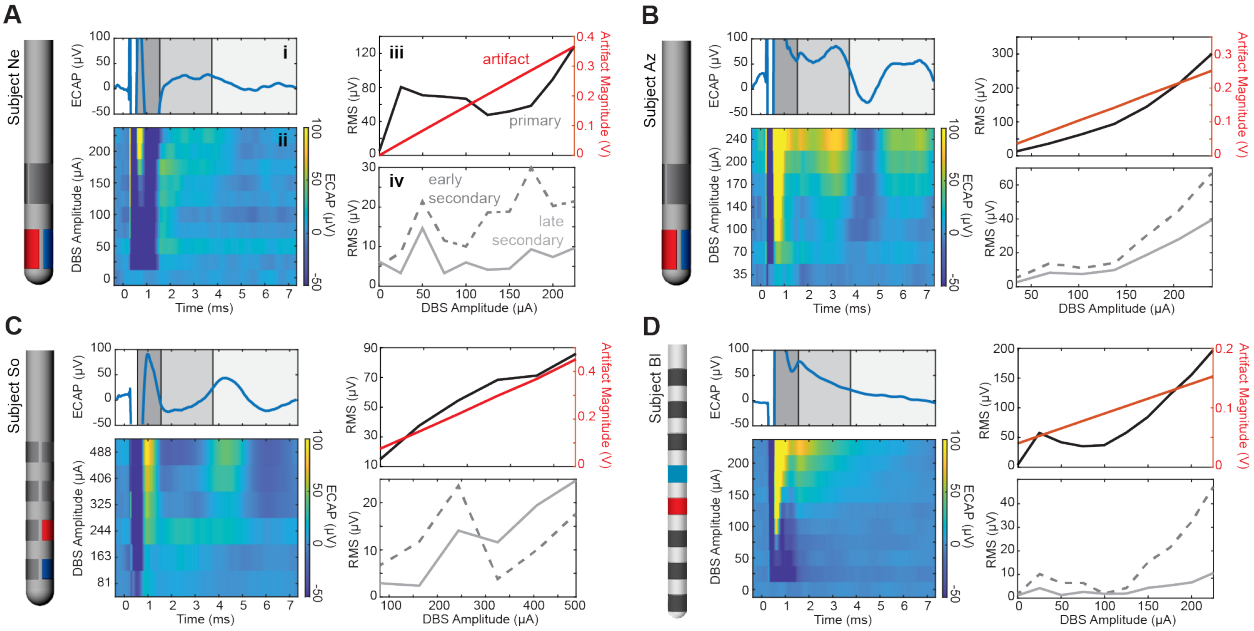

Figure 4. ECAP responses to varying stimulation amplitudes. (A-D, left) Lead diagrams for each subject with stimulation electrode shown in red and recording site shown in blue. Shown are stimulation/recording configurations of 2B/2C for subject Az; 2B/2C for subject Ne; 2B/1B for subject So; 4/5 for subject Bl. (A-D, part i) Example averaged ECAP response to the highest stimulation amplitude for a single recording and stimulation site in the MPTP state of each subject. (A-D, part ii) Example averaged ECAP response to varying stimulation current amplitudes for a single recording and stimulation site configuration. (A-D, part iii) RMS values of epochs defined as stimulation artifact and primary feature across stimulation amplitudes. (A-D, part iv) Secondary feature RMS values compared to stimulation amplitude.

ECAP response features also followed classical strength duration curves at 82.5% and 100% of side effect threshold amplitudes (**Fig. 5**). Due to differences in side effect thresholds between subjects, shorter pulse widths could achieve much higher stimulation amplitudes in subject So, making evoked responses much stronger for longer pulse widths when normalized to stimulation amplitude (**Fig. 5**). Subject Az had a smaller difference (~450µA) in stimulation amplitudes between the shortest and the longest pulse widths, while subject So had a greater difference (~700µA), which may account for the inconsistency in the relative effectiveness of the different pulse widths at 82.5% of threshold for each subject.

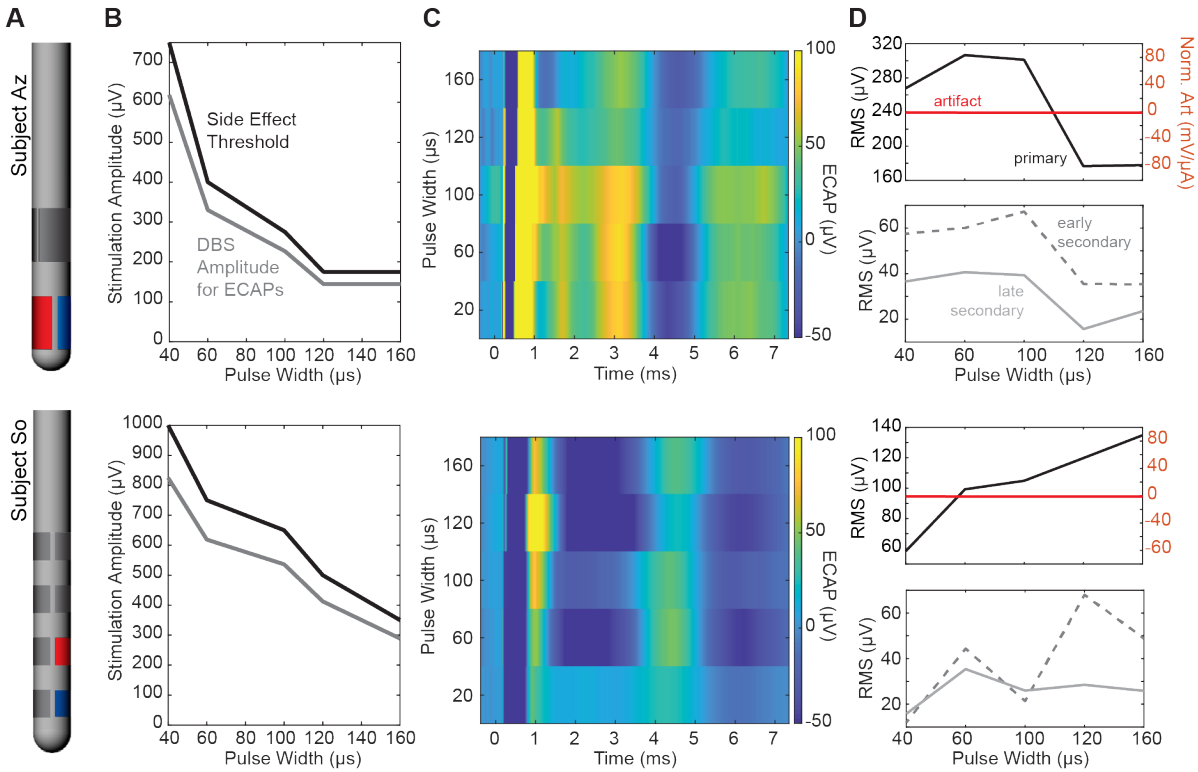

Figure 5. ECAP responses to varying pulse widths. (A) Lead configurations for each subject with the stimulating electrode shown in red and the recording site shown in blue: 2B/2C for subject Az and 2B/1B for subject So. (B) Strength-duration curves for side effect thresholds and stimulation amplitudes at 82.5% of the side effect thresholds across pulse widths. (C) Example ECAP responses in the MPTP state to varying stimulation pulse width at 82.5% of side effect thresholds. (D) Feature RMS values and normalized stimulation artifact amplitude for each pulse width tested.

3.3. Spatial Heterogeneity of ECAP Features

The spatial ECAP response differences were readily visible and distinguished by a simple linear classifier (**Fig. 6**). This classifier, trained on all subjects, was capable of correctly determining the stimulation and recording sites as being either both in the STN or both in ThF with 95.2% accuracy (measured using the leave-one-out method). Furthermore, when trained on all data from three subjects and tested using data solely from a fourth, the classifier was able to accurately determine the locations of the fourth subject's electrodes with 75% (subject Az), 81.25% (subject So), 100% (subject Bl), and 93.3% (subject Ne) accuracy. This suggests that the DBS ECAP response in both directional and ring electrode configurations can be used to gain an understanding of implant location and help direct clinicians in choosing DBS parameters to test when targeting a specific region, and that such a model may be generalizable across subjects. The perfect accuracy in subject Bl's case was likely due to the smaller number of samples relative to the other subjects. The main determining feature across all subjects was the primary feature amplitude (**Fig. 6**), though there were also visible differences in secondary features in subjects Az and So.

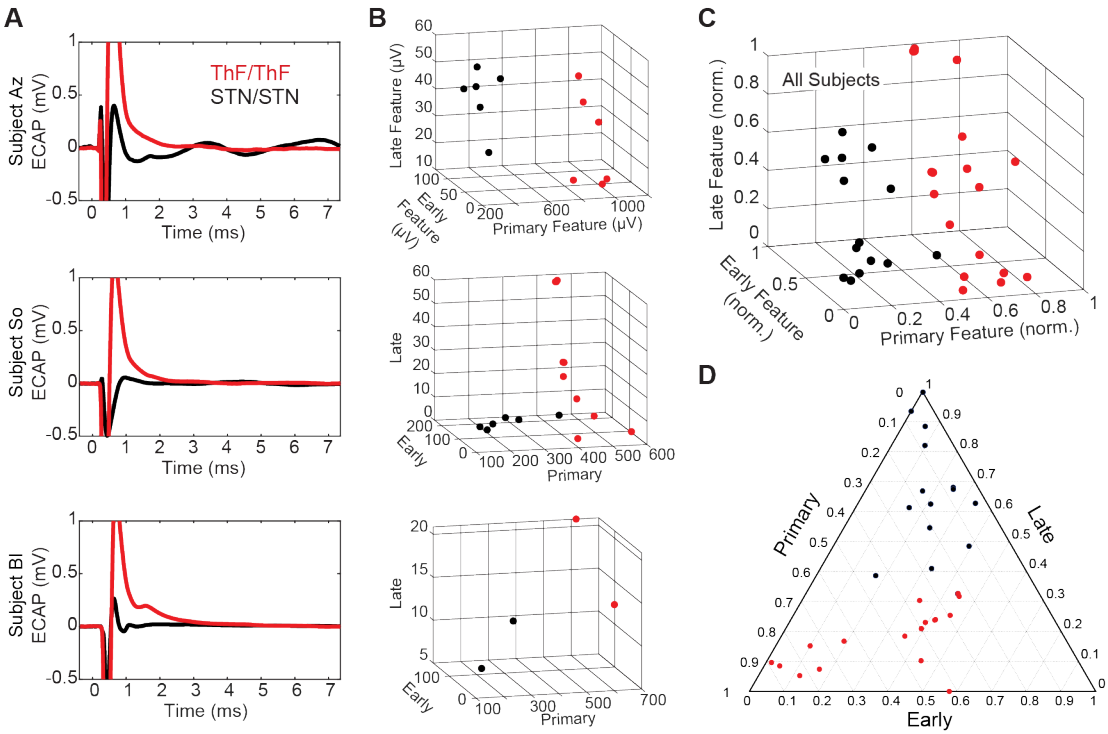

Figure 6. Classification of ECAP responses within and dorsal to the STN. (A) Example ECAP responses for stimulation/recording with STN/STN and ThF/ThF from subjects Az, So, and Bl. Subject Ne was excluded from this figure as all her electrodes were within the STN. Stimulation amplitudes in each case are similar but not identical within each subject. (B) Plots of three of each subjects' features used by the classifier showing separability of spatial categories (STN/STN, ThF/ThF) in feature space. (C) RMS values (normalized within subjects) plotted together to show separability of spatial categories in feature space. (D) Data plotted on ternary axes for easier visibility.

Changes spatial and temporal arrangement of dipoles generated by DBS were visible across stimulation amplitudes (**Fig. 7**). At low amplitude, all recording channels had similar ECAP responses, but as stimulation amplitude increases, a dipole between the STN and thalamo-fascicular recording sites appeared, noted by the flipping of polarity of certain ECAP features between those locations. The strength of the dipole increased with increased stimulation amplitude, while the time delay of the dipole also changed in the recording. Upon reaching or exceeding side effect threshold (650μA in this case), the dipole became unstable or moved in space such that all recording channels grew together once more, though with differing ECAP response amplitudes.

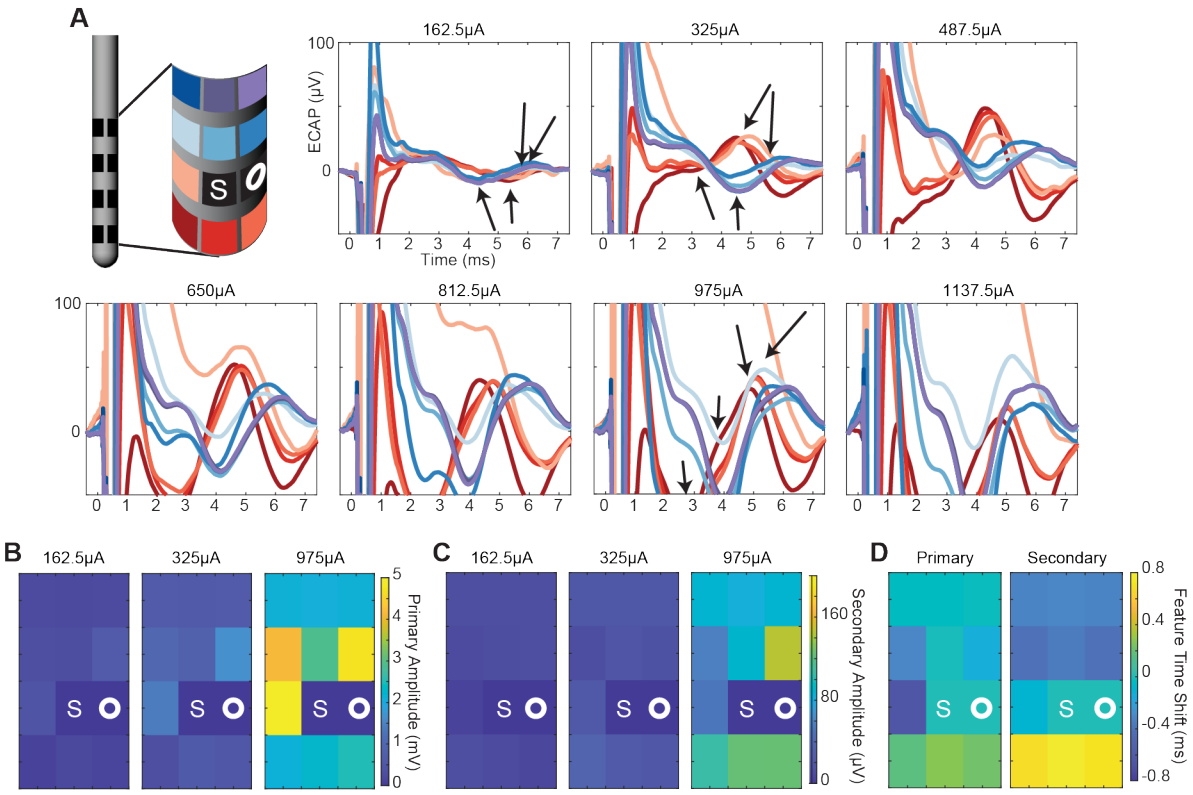

Figure 7. Spatiotemporal changes in ECAP features with increasing stimulation amplitude. (A) ECAP responses in each recording channel and a single stimulation site (e5) to increasing stimulation amplitudes (applied in a randomized order over a single recording session) in subject So in the MPTP state. Side effect threshold for the stimulation site was 650µA. A dipole was present between rows 1/2 (reds) and 3/4 (blues) from 325µA to 812.5µA. Color grid represents positions of recording sites on lead (unwrapped for 2D representation). (B) Primary feature and (C) secondary feature peak-trough difference for each recording site over three stimulation amplitudes. Arrows in part A indicate which peaks and troughs were used for the secondary feature. (D) Change in primary and secondary feature time of occurrence (average of the timing of the peak and trough in each feature) for each recording site between the 325µA stimulation amplitude and 975µA stimulation amplitude. A positive value signifies the feature appeared later in the response and a negative value means the feature appeared earlier in the response to 975µA stimulation. Secondary features appeared later in the response for STN sites and earlier in the response for ThF sites at 975µA than at 325µA. O marker indicates an open channel, and S marker indicates the stimulation site.

4. Discussion

This study investigated the spatial and temporal features of ECAPs collected within and around the STN in four parkinsonian non-human primates. While previous studies using DBS leads with macroscale ring electrodes have noted that the presence and prominence of ECAP features may have some association with therapeutic effectiveness of DBS on parkinsonian motor signs [17,20], how these features vary with amplitude, pulse width, electrode configuration, and placement in the

STN region has not been well studied. This study leveraged directional DBS leads – enabling multi-channel recordings within and dorsal to the STN in the same subject – as well as post-mortem histological verification of the position and orientation of each electrode contact to shed new light on these relationships.

4.1. Dependence of ECAP Features on Stimulation Parameters

The ECAP features (a) followed a sigmoidal intensity curve with respect to stimulation amplitude; (b) had strength-duration curve relationships between stimulation amplitude and pulse width; and (c) varied by subject and stimulation/recording electrode configurations. Findings (a) and (b) provide continued support for the neurobiological basis of ECAPs, while finding (c) indicates a need to use subject-agnostic analysis methods and the potential usefulness of ECAP responses in determining lead implant locations using multi-subject models. Traditionally, ECAP features have been viewed as having specific peak and trough features [1,2,4,17,26]. However, in this study, the timing, location, and number of features varied depending on stimulation amplitude and electrode configuration, lead geometry, and implant location. Using time ranges rather than specific points when calculating ECAP features allowed for more broadly applicable data analyses such as the use of summary statistics like RMS values, rather than peak-to-trough amplitudes or prominences.

4.2. Spatial Classification of Electrode Location based on ECAP Features

Previous ECAP studies have relied on macroscale electrodes and bipolar recording configurations with two electrodes guarding a center stimulating electrode [2,17,26]. In this study, using directional DBS leads, ECAP features were shown to exhibit a spatial heterogeneity both between rows and within rows, which is consistent with the finer-scale spatial resolution of LFPs [27]. In addition, this study showed that monopolar recordings of ECAP responses had visually separable features between the STN and regions dorsal to the STN, most prominently observed in the primary features, and these features enabled classifying electrode location (within STN or dorsal to STN) with high accuracy across subjects. The ability of a linear classifier to accurately predict where a stimulation and recording site pair are located could be useful for programming DBS systems especially as DBS lead designs become more complex and clinical monopolar reviews take longer to complete. Studies have shown that stimulation targeting specific regions about the STN can be helpful in the programming process. For example, the dorsal region above STN can be beneficial for the cardinal motor signs of PD including rigidity and bradykinesia [28], but also helpful for suppressing stimulation-induced dyskinesias [19]. Though the ECAP response data did not support a method to determine DBS lead orientation, additional subjects and recordings spanning a broader set of implant locations would be helpful to tease apart the neuroanatomical origins of differences in directional ECAP responses.

4.4. Limitations

The use of alternating polarity stimulation as a means of canceling stimulation artifact meant the stimulation parameters differed slightly from what is used clinically. However, a previous study using artifact removal hardware for thalamic ECAP recordings suggests that the anodic-leading and cathodic-leading ECAP responses and therapeutic effect on tremor are largely similar [26]. Additionally, some, but not all, recordings contained high-frequency noise in the 0.7-1.5 kHz range, which necessitated offline filtering. While the approach removed most of the high-

frequency noise, some recordings still had a small residual noise level remaining. By employing analysis techniques such as calculation of RMS values as our feature amplitude metric, we reduced the effect that any residual noise had on the analysis, since the noise was of a high enough frequency to have multiple periods within a given feature window.

5. Conclusion

This study found several principles that govern ECAP responses to DBS targeted within and around the STN. Increased stimulation amplitude or pulse width primarily affected the amplitude of ECAP features so long as the stimulation parameter exceeded a threshold to produce a detectable response feature. In contrast, variation in stimulation and recording site configurations had a significant effect on when and what features were present in the ECAP response. Importantly, primary feature amplitude provided a means to distinguish electrode contacts within or dorsal to the STN, which will be useful for guiding the programming of STN-DBS systems.

Funding sources
This study was supported by the NIH-NINDS under grants R01-NS094206, P50-NS098573, P50-NS123109, R01-NS037019, R37-NS077657, R01-NS058945.

Acknowledgements
We would like to thank the Neuromodulation Research and Technology Lab for helpful comments in preparation of this manuscript, and the RAR and veterinary staff at the University of Minnesota.

CRediT authorship contribution statement
Joshua Rosing: Conceptualization, Methodology, Software, Validation, Formal analysis, Investigation, Data Curation, Writing – original draft, Writing – review & editing, Visualization. **Alex Doyle:** Investigation, Writing – review & editing, Visualization. **AnneMarie Brinda:** Investigation, Writing – review & editing, Visualization. **Madeline Blumenfeld:** Investigation, Writing – review & editing. **Emily Lecy:** Investigation, Writing – review & editing. **Chelsea Spencer:** Investigation, Writing – review & editing. **Joan Dao:** Investigation, Writing – review & editing. **Jordan Krieg:** Investigation, Writing – review & editing. **Kelton Wilmerding:** Investigation, Writing – review & editing. **Disa Sullivan:** Investigation, Writing – review & editing. **Sendréa Best:** Investigation, Writing – review & editing. **Biswaranjan Mohanty:** Investigation, Writing – review & editing. **Jing Wang:** Investigation, Writing – review & editing. **Luke A. Johnson:** Conceptualization, Investigation, Resources, Writing – review & editing, Supervision, Project administration. **Jerrold L. Vitek:** Conceptualization, Resources, Writing – review & editing, Supervision, Project administration, Funding acquisition. **Matthew D. Johnson:** Conceptualization, Methodology, Validation, Formal analysis, Writing – original draft, Writing – review & editing, Visualization, Supervision, Project administration, Funding acquisition.

Declaration of competing interest
Authors do not report biomedical financial interests or potential conflicts of interest with this study.

References

[1] Kent AR, Grill WM. Neural origin of evoked potentials during thalamic deep brain stimulation. J Neurophysiol 2013;110:826–43. https://doi.org/10.1152/jn.00074.2013.
[2] Schmidt SL, Brocker DT, Swan BD, Turner DA, Grill WM. Evoked potentials reveal neural circuits engaged by human deep brain stimulation. Brain Stimulation 2020;13:1706–18. https://doi.org/10.1016/j.brs.2020.09.028.
[3] Buzsáki G, Anastassiou CA, Koch C. The origin of extracellular fields and currents — EEG, ECoG, LFP and spikes. Nat Rev Neurosci 2012;13:407–20. https://doi.org/10.1038/nrn3241.
[4] Kent AR, Grill WM. Recording evoked potentials during deep brain stimulation: development and validation of instrumentation to suppress the stimulus artefact. J Neural Eng 2012;9:036004. https://doi.org/10.1088/1741-2560/9/3/036004.
[5] Cohen LT, Richardson LM, Saunders E, Cowan RSC. Spatial spread of neural excitation in cochlear implant recipients: comparison of improved ECAP method and psychophysical forward masking. Hearing Research 2003;179:72–87. https://doi.org/10.1016/S0378-5955(03)00096-0.
[6] Tang Q, Benítez R, Zeng F-G. Spatial channel interactions in cochlear implants. J Neural Eng 2011;8:046029. https://doi.org/10.1088/1741-2560/8/4/046029.
[7] Parker JL, Shariati NH, Karantonis DM. Electrically evoked compound action potential recording in peripheral nerves. Bioelectronics in Medicine 2018;1:71–83. https://doi.org/10.2217/bem-2017-0005.
[8] Parker JL, Obradovic M, Hesam Shariati N, Gorman RB, Karantonis DM, Single PS, et al. Evoked Compound Action Potentials Reveal Spinal Cord Dorsal Column Neuroanatomy. Neuromodulation: Technology at the Neural Interface 2020;23:82–95. https://doi.org/10.1111/ner.12968.
[9] Russo M, Brooker C, Cousins MJ, Taylor N, Boesel T, Sullivan R, et al. Sustained Long-Term Outcomes With Closed-Loop Spinal Cord Stimulation: 12-Month Results of the Prospective, Multicenter, Open-Label Avalon Study. Neurosurgery 2020;87:E485–95. https://doi.org/10.1093/neuros/nyaa003.
[10] Parker JL, Karantonis DM, Single PS, Obradovic M, Laird J, Gorman RB, et al. Electrically Evoked Compound Action Potentials Recorded From the Sheep Spinal Cord. Neuromodulation: Technology at the Neural Interface 2013;16:295–303. https://doi.org/10.1111/ner.12053.
[11] Jeon EK, Brown CJ, Etler CP, O'Brien S, Chiou L-K, Abbas PJ. Comparison of Electrically Evoked Compound Action Potential Thresholds and Loudness Estimates for the Stimuli Used to Program the Advanced Bionics Cochlear Implant. J Am Acad Audiol 2010;21:016–27. https://doi.org/10.3766/jaaa.21.1.3.
[12] Miller CA, Brown CJ, Abbas PJ, Chi S-L. The clinical application of potentials evoked from the peripheral auditory system. Hearing Research 2008;242:184–97. https://doi.org/10.1016/j.heares.2008.04.005.
[13] Adenis V, Gourévitch B, Mamelle E, Recugnat M, Stahl P, Gnansia D, et al. ECAP growth function to increasing pulse amplitude or pulse duration demonstrates large inter-animal variability that is reflected in auditory cortex of the guinea pig. PLOS ONE 2018;13:e0201771. https://doi.org/10.1371/journal.pone.0201771.
[14] Gärtner L, Lenarz T, Büchner A. Fine-grain recordings of the electrically evoked compound action potential amplitude growth function in cochlear implant recipients. Biomed Eng Online 2018;17:140. https://doi.org/10.1186/s12938-018-0588-z.

[15] Finn WE, LoPresti PG. Wavelength and intensity dependence of retinal evoked responses using in vivo optic nerve recording. IEEE Transactions on Neural Systems and Rehabilitation Engineering 2003;11:372–6. https://doi.org/10.1109/TNSRE.2003.819928.
[16] Maynard et al. Nitric oxide modulates light-evoked compound action potentials in the intact rabbit retina. Lippincott-Raven Publishers 1995;6:850–2.
[17] Gmel GE, Hamilton TJ, Obradovic M, Gorman RB, Single PS, Chenery HJ, et al. A new biomarker for subthalamic deep brain stimulation for patients with advanced Parkinson's disease--a pilot study. J Neural Eng 2015;12:066013. https://doi.org/10.1088/1741-2560/12/6/066013.
[18] Somers B, Long CJ, Francart T. EEG-based diagnostics of the auditory system using cochlear implant electrodes as sensors. Sci Rep 2021;11:5383. https://doi.org/10.1038/s41598-021-84829-y.
[19] Goftari M, Kim J, Johnson E, Patriat R, Palnitkar T, Harel N, et al. Pallidothalamic tract activation predicts suppression of stimulation-induced dyskinesias in a case study of Parkinson's disease. Brain Stimulation: Basic, Translational, and Clinical Research in Neuromodulation 2020;13:1821–3. https://doi.org/10.1016/j.brs.2020.09.022.
[20] Sanabria DE, Johnson LA, Yu Y, Busby Z, Nebeck S, Zhang J, et al. Real-time suppression and amplification of frequency-specific neural activity using stimulation evoked oscillations. Brain Stimulation: Basic, Translational, and Clinical Research in Neuromodulation 2020;13:1732–42. https://doi.org/10.1016/j.brs.2020.09.017.
[21] Brinda AK, Doyle AM, Blumenfeld M, Krieg J, Alisch JSR, Spencer C, et al. Longitudinal analysis of local field potentials recorded from directional deep brain stimulation lead implants in the subthalamic nucleus. J Neural Eng 2021;18:046050. https://doi.org/10.1088/1741-2552/abfc1c.
[22] Vitek JL, Johnson LA. Understanding Parkinson's disease and deep brain stimulation: Role of monkey models. Proceedings of the National Academy of Sciences 2019;116:26259–65. https://doi.org/10.1073/pnas.1902300116.
[23] Miocinovic S, Parent M, Butson CR, Hahn PJ, Russo GS, Vitek JL, et al. Computational analysis of subthalamic nucleus and lenticular fasciculus activation during therapeutic deep brain stimulation. J Neurophysiol 2006;96:1569–80. https://doi.org/10.1152/jn.00305.2006.
[24] Imbert C, Bezard E, Guitraud S, Boraud T, Gross CE. Comparison of eight clinical rating scales used for the assessment of MPTP-induced parkinsonism in the Macaque monkey. Journal of Neuroscience Methods 2000;96:71–6.
[25] Meissner W, Leblois A, Hansel D, Bioulac B, Gross CE, Benazzouz A, et al. Subthalamic high frequency stimulation resets subthalamic firing and reduces abnormal oscillations. Brain 2005;128:2372–82. https://doi.org/10.1093/brain/awh616.
[26] Kent AR, Swan BD, Brocker DT, Turner DA, Gross RE, Grill WM. Measurement of evoked potentials during thalamic deep brain stimulation. Brain Stimul 2015;8:42–56. https://doi.org/10.1016/j.brs.2014.09.017.
[27] Zhang S, Connolly AT, Madden LR, Vitek JL, Johnson MD. High-resolution local field potentials measured with deep brain stimulation arrays. J Neural Eng 2018;15:046019. https://doi.org/10.1088/1741-2552/aabdf5.
[28] Butson CR, Cooper SE, Henderson JM, McIntyre CC. Patient-Specific Analysis of the Volume of Tissue Activated During Deep Brain Stimulation. Neuroimage 2007;34:661–70. https://doi.org/10.1016/j.neuroimage.2006.09.034.